Development/Plasticity/Repair

Long-Term Seizure Suppression and Optogenetic Analyses of Synaptic Connectivity in Epileptic Mice with Hippocampal Grafts of GABAergic Interneurons

Katharine W. Henderson,[1]* Jyoti Gupta,[1]* Stephanie Tagliatela,[1,2] Elizabeth Litvina,[1,3] XiaoTing Zheng,[1] Meghan A. Van Zandt,[1] Nicholas Woods,[1] Ethan Grund,[1] Diana Lin,[1] Sara Royston,[1,4] Yuchio Yanagawa,[5] Gloster B. Aaron,[1] and Janice R. Naegele[1]

[1]Department of Biology, Program in Neuroscience and Behavior, Hall-Atwater Laboratory, Wesleyan University, Middletown, Connecticut 06459-0170, [2]Department of Brain and Cognitive Sciences, Massachusetts Institute of Technology, Cambridge, Massachusetts 02139-4307, [3]Department of Neurobiology, Harvard Medical School, Boston, Massachusetts 02115-5701, [4]Medical Scholars Program, Neuroscience Program, University of Illinois Urbana-Champaign, Urbana, Illinois 61801-6210, and [5]Department of Genetic and Behavioral Neuroscience, Gunma University Graduate School of Medicine, Japan and Japan Science and Technology Agency, CREST, Tokyo 102-0075, Japan

Studies in rodent epilepsy models suggest that GABAergic interneuron progenitor grafts can reduce hyperexcitability and seizures in temporal lobe epilepsy (TLE). Although integration of the transplanted cells has been proposed as the underlying mechanism for these disease-modifying effects, prior studies have not explicitly examined cell types and synaptic mechanisms for long-term seizure suppression. To address this gap, we transplanted medial ganglionic eminence (MGE) cells from embryonic day 13.5 VGAT-Venus or VGAT-ChR2-EYFP transgenic embryos into the dentate gyrus (DG) of adult mice 2 weeks after induction of TLE with pilocarpine. Beginning 3–4 weeks after status epilepticus, we conducted continuous video-electroencephalographic recording until 90–100 d. TLE mice with bilateral MGE cell grafts in the DG had significantly fewer and milder electrographic seizures, compared with TLE controls. Immunohistochemical studies showed that the transplants contained multiple neuropeptide or calcium-binding protein-expressing interneuron types and these cells established dense terminal arborizations onto the somas, apical dendrites, and axon initial segments of dentate granule cells (GCs). A majority of the synaptic terminals formed by the transplanted cells were apposed to large postsynaptic clusters of gephyrin, indicative of mature inhibitory synaptic complexes. Functionality of these new inhibitory synapses was demonstrated by optogenetically activating VGAT-ChR2-EYFP-expressing transplanted neurons, which generated robust hyperpolarizations in GCs. These findings suggest that fetal GABAergic interneuron grafts may suppress pharmacoresistant seizures by enhancing synaptic inhibition in DG neural circuits.

Key words: **EEG; epilepsy; GABA; seizures; transplantation**

Introduction

Severe, pharmacoresistant seizures in temporal lobe epilepsy (TLE) are a significant medical problem. Cellular, genetic, and epigenetic mechanisms have been proposed to account for epileptogenesis, including a loss of functional inhibition of dentate gyrus (DG) granule cells (GCs). Hilar GABAergic interneuron cell death induced by prolonged status epilepticus (SE) is a common finding in patients with intractable seizures and mesial TLE (MTLE; de Lanerolle et al., 1989; Mathern et al., 1995; Swartz et al., 2006; Tóth et al., 2010). Despite compensatory sprouting by surviving interneurons, diminished inhibition in both the hippocampus and entorhinal cortex characterize rodent pilocarpine models of TLE (Kumar and Buckmaster, 2006; Zhang et al., 2009; Thind et al., 2010; Peng et al., 2013). Additional epilepsy-related neuropathological changes, including abnormal GC migration and hypertrophy, and concomitant mossy fiber sprouting (MFS), develop during epileptogenesis (Tauck and Nadler, 1985; Nadler, 2003; Danzer et al., 2010; Buckmaster and Lew, 2011; Murphy et al., 2011).

To correct deficits in GABAergic neurotransmission in TLE, GABAergic cell transplantation has been tested for reducing seizures. Implanting GABA-releasing cell lines was found to elevate seizure thresholds through nonsynaptic mechanisms (Gernert et al., 2002; Thompson, 2009). Additional studies transplanting GABAergic progenitors from the embryonic forebrain medial

Received Dec. 30, 2013; revised July 22, 2014; accepted Aug. 28, 2014.

Author contributions: J.R.N. designed research; K.W.H., J.G., S.T., E.L., X.T.Z., M.A.V.Z., N.W., E.G., D.L., and S.R. performed research; K.W.H., J.G., S.T., E.L., X.T.Z., M.A.V.Z., N.W., E.G., D.L., and S.R. analyzed data; K.W.H., J.G., X.T.Z., M.A.V.Z., and J.R.N. wrote the paper.

This work was supported by NINDS grant R15NS072879-01A1, Connecticut Stem Cell Established Investigator Grant, and a Challenge Award from Citizens United for Research in Epilepsy (J.R.N.). We thank Dr Atsushi Miyawaki of RIKEN Brain Science Institute, Wako, Saitama, Japan for the pCS2-Venus plasmid and Manolis Kaparakis and Jen Rose, Quantitative Analysis Center, Wesleyan University, for assistance with statistical analyses.

The authors declare no competing financial interests.

*K.W.H. and J.G. contributed equally to this work.

Correspondence should be addressed to Janice R. Naegele, Wesleyan University, 52 Lawn Avenue, Middletown, CT 06459. E-mail: jnaegele@wesleyan.edu.

DOI:10.1523/JNEUROSCI.0005-14.2014

Copyright © 2014 the authors 0270-6474/14/3413492-13$15.00/0

ganglionic eminence (MGE) showed their capacity to migrate and differentiate into GABAergic interneurons (Wichterle et al., 1999; Alvarez-Dolado et al., 2006; Calcagnotto et al., 2010a,b). When transplanted into the adult rodent hippocampus, MGE cells reduced limbic seizures (Waldau et al., 2010; Hunt et al., 2013), increased inhibitory postsynaptic currents, and raised seizure thresholds (Calcagnotto et al., 2010a; Zipancic et al., 2010).

To advance cell-based treatments for patients with TLE or other diseases, mouse or human embryonic stem cell (ESC)-GABAergic interneuron transplantation has been studied (Tyson and Anderson, 2014). ESC-derived GABAergic progenitors transplanted into the hippocampus were shown to integrate synaptically and exhibit many of the morphological and physiological attributes of endogenous interneurons (Carpentino et al., 2008; Hartman et al., 2010; Maisano et al., 2012). Large-scale, *in vitro* production of human forebrain GABAergic interneurons from ESCs or induced pluripotent stem cells (iPSCs) recently became possible, based on a more complete understanding of combinations and sequences of growth factors and signaling molecules required for specifying interneuron fates (Kriegstein and Alvarez-Buylla, 2009; Germain et al., 2013; Maroof et al., 2013; Nicholas et al., 2013). Despite these advances, GABAergic interneuron cell therapy for patients with intractable MTLE is currently unfeasible, due to the protracted differentiation time required for human neurons and potential for tumors. Moreover, whether functional inhibitory circuits can be established for enduring seizure suppression is not yet known.

We therefore investigated long-term suppression of spontaneous recurrent seizures (SRS) following transplantation of fetal MGE cells into mice with pilocarpine-induced TLE. During the 2 month period of continuous video-electroencephalographic (V-EEG) monitoring, mice with DG transplants had significantly fewer and milder seizures, compared with controls. Seizure suppression correlated with differentiation of the transplants and synapse formation onto GCs. We further show transplant-mediated synaptic inhibition of GCs by optogenetic stimulation of ChR2-EYFP-expressing interneuron transplants combined with patch-clamp electrophysiological recordings (Wang et al., 2007; Schoenenberger et al., 2011; Peng et al., 2013).

Materials and Methods

Pilocarpine and drug administration. All animal procedures followed protocols approved by the Wesleyan University Institutional Animal Care and Use Committee. Male C57BL/6 mice (Harlan Laboratories; 3–4 weeks of age) were handled daily and singly housed in Wesleyan University animal facilities for 1 to 2 weeks before seizure induction. Seizures were induced when the mice were 5–6 weeks of age and weighed 18–22 g. Seizures were initiated 30 min following injection of methyl atropine (Sigma-Aldrich, 17 mg/kg, i.p.) or scopolamine methyl bromide (Sigma-Aldrich, 17 mg/kg, i.p.) by systemic injection of pilocarpine hydrochloride (Sigma-Aldrich, 180 mg/kg, i.p.). Mice that did not show characteristic seizure behavior within 30 min received supplementary doses of pilocarpine. Seizure incidence and grade were scored with a modified Racine scale (Shibley and Smith, 2002). Mice that reached SE and continued to exhibit stage 1 or 2 behavior for 1 h were selected for further study, and their seizures were attenuated with injections of midazolam (Henry Schein, 20 mg/kg, i.p.). Mice were injected daily with 5% dextrose in lactated Ringer's solution (Henry Schein, 1 ml, i.p.) until they recovered.

MGE dissection and transplantation. The two transgenic lines used to harvest MGE cells were VGAT-Venus mice (Line no. 39; Wang et al., 2009) or VGAT-ChR2(H134R)-EYFP from Jackson Laboratories (Zhao et al., 2011). Embryonic day (E)13.5 pups from our breeding colony at Wesleyan University were harvested from timed pregnant dams killed via cervical dislocation.

Fluorescent embryos were identified after removal from the pregnant dam by viewing them under specialized goggles (FHS/F-01 goggles equipped with FHS/EF-2G2 emission filters, Biological Laboratory Equipment Maintenance and Service Ltd.). Using the anatomical criteria previously described (Xu et al., 2004), the MGE were carefully isolated by free-hand whole-brain dissection in cold Hank's Balanced Salt Solution (HBSS) without calcium or magnesium, using a Zeiss Stemi 2000-C. The cells were treated with 0.25% trypsin (Sigma-Aldrich) in HBSS for 12 min at 37°C. Enzymatic digestion was terminated by addition of trypsin inhibitor (Sigma-Aldrich) in HBSS. Cells were triturated with fire-polished glass pipettes in HBSS with trypsin inhibitor. Cells were centrifuged and suspended at a concentration of 1×10^5 cells/μl in transplantation media consisting of: 418 ml DMEM/F12 (Invitrogen), 10 ml 30% glucose, 7.5 ml 7.5% $NaHCO_3$, 2.5 ml 1 M HEPES, 5 ml 200 mM glutamine (Sigma-Aldrich), 5 ml penicillin-streptomycin (Sigma-Aldrich), 20 μl heparin (Sigma-Aldrich), 2 ml Fungizone (Invitrogen), 50 ml hormone mix (8 ml 30% glucose, 6 ml 7.5% $NaHCO_3$, 2 ml 1 M HEPES, 400 mg transferrin, 100 mg insulin, 36 ml ddH_2O, 38.6 mg putrescine in 40 ml ddH_2O, 40 μl selenium, and 40 μl progesterone), supplemented with 0.15% pan-caspase inhibitor (Promega), 0.2% B27, 50 ng/nL fibroblast growth factor, and 187.5 ng/ml epidermal growth factor.

Transplantation of MGE-derived interneuron progenitors into the DG or lateral entorhinal cortex (LEC) was performed by stereotaxic injections, two weeks following SE. Controls were injected with media alone or dead cells suspended in complete media. The mice were anesthetized for the duration of stereotaxic surgery by isoflurane gas inhalation (David Kopf Instruments, VetEquip, Harvard Apparatus). Bilateral injections were made into the hilus of the DG (stereotaxic coordinates AP −2.5 mm, ML ± 2.1 mm, DV 2.0 mm) or the LEC (coordinates: AP −3.2 mm, ML ± 4.2 mm, DV 5.0 mm) via a 5 μl glass Hamilton syringe outfitted with a 30° bevel-tip needle. A total of 1×10^5 cells were suspended in 1 μl of media and injected at each site over 5 min. The needle remained in place for an additional 5 min before it was withdrawn from the tissue. For LEC transplants, cells were injected in volumes of 0.1–0.2 μl over a 1 mm dorsoventral distance as the needle was slowly withdrawn. Incisions were closed with Vetbond tissue adhesive (3M), and the mice were maintained on a heating pad before they were returned to their cages.

Electrode implantation. One week following MGE cell transplantation, we commenced long-term V-EEG recordings using subdural electrodes consisting of a six-position socket dual row base with 0.05 cm spacing (Digi-Key) and silver wire pins. For the head-electrode implantation surgery, the mice were anesthetized with isoflurane gas and placed in the stereotaxic device. Screws (3/32 inch, Plastics One, 00-9653/32) were placed in predrilled holes on the surface of the skull anterior to bregma and posterior to lambda. One silver wire electrode pin was wrapped around each of the screws, and Silver Print II (Allied Electronics, 796-2036) was applied. These two wires were used as reference (anterior) and ground (posterior). Four additional electrodes were placed on the cortical surface at AP coordinates −1.5 mm and −3.0 mm and ML coordinates ± 2.5 mm and ± 3.0 mm. The exposed skull was covered with a cyanoacrylate resin (Locktite Liquid, Henkel), and a dental acrylic cap was made (Lang Dental Manufacturing) to fasten the electrodes in place.

V-EEG recording. Electrodes were surgically implanted ~3 weeks after SE and the following day, the mice were introduced into 12-inch diameter cylindrical Plexiglas chambers for chronic V-EEG recordings for ~100–140 d after SE (up to 120 d of continuous V-EEG recordings). Mice had free access to food, nesting materials, and water at all times and were maintained on a 12 h light/dark schedule throughout testing. The head electrode was connected to a computer (Dell) via a customized connector wire, a swivel (Plastics One, SL6C), and a six-channel cable (Plastics One). Data were recorded and analyzed with either a Stellate Harmonie V-EEG system (Natus Technology) or a three-channel system with Sirenia software (Pinnacle Technology). The sensitivity was set at 50 μV/mm and low (0.3 Hz) and high (70 Hz) frequency filters were used throughout the experiment. Continuous Mpeg4 videos were time synchronized with the EEG recordings. The software algorithm for seizure detection used line length deviations from standard baseline recordings as well as spike frequency. Ictal events detected by the software were also manually confirmed offline. Seizure severity was scored behaviorally

from V-EEG recordings by an observer using the Racine scale and classified as localized (Racine scale 1–2) or generalized (Racine scale 3–6). Statistical analyses were performed with STATA statistical software (v13.1, STATA) to compare the effects of treatment (media injections vs MGE cell transplants in the hilus) on the average number of seizures per treatment group for three consecutive 20 d intervals during a 60 d period of continuous V-EEG monitoring (40–60, 61–80, and 81–100 d) using a repeated-measures ANOVA. Based on pilot studies, these three intervals were selected to capture the effects of MGE transplants on SRS during the initial 3–4 week period after transplantation when the cells were differentiating, and the two successive periods during which our transplants appeared to have integrated synaptically and showed good survival. A repeated-measures ANOVA was also used to compare the effects of treatment on total seizure duration/d during three time periods within a 60 d V-EEG monitoring period. Statistical comparisons of treatment on seizure severity examined the average number of seizures for Racine stages 1–2 and stages 3–6 per group, using a Student's *t* test.

Hippocampal slice electrophysiology. Whole-cell patch-clamp recordings were made in brain slices 90–130 d after injection of media, dead cells, or MGE-derived GABAergic progenitors. The slices were obtained from adult C57BL/6 TLE mice at ~19–24 weeks of age. The mice were deeply anesthetized with an injection of ketamine/xylazine (120 mg/kg ketamine, 10 mg/kg xylazine, i.p.), and brains were rapidly removed and transferred to cold, oxygenated, high sucrose ACSF (27.07 mM $NaHCO_3$, 1.5 mM NaH_2PO_4, 1 mM $CaCl_2$, 3 mM $MgSO_4$, 2.5 mM KCl, 222.14 mM sucrose). Thick sections (350 μm) were subsequently cut on a Vibratome (Leica, VT1000S) in the horizontal plane from ventral to dorsal. Electrophysiology was performed in sections corresponding to atlas plates 148–156 (Paxinos and Franklin, 2008).

Slices were incubated for 1 h in a holding chamber containing oxygenated ACSF (125 mM NaCl, 1 mM $CaCl_2$, 3 mM $MgSO_4$, 1.25 mM NaH_2PO_4, 25 mM $NaHCO_3$, 2.5 mM KCl, 25 mM glucose, 3 mM *myo*-inositol, 2 mM Na-pyruvate, 0.4 mM ascorbic acid) before being placed in the recording chamber. While recording, slices were continuously perfused with heated (34°C) and oxygenated ACSF (125 mM NaCl, 1.5 mM $CaCl_2$, 1.0 mM $MgSO_4$, 1.25 mM NaH_2PO_4, 25 mM $NaHCO_3$, 3.5 mM KCl, 25 mM glucose, 3 mM *myo*-inositol, 2 mM Na pyruvate, 0.4 mM ascorbic acid). Patch pipettes were pulled (Sutter Instrument Company, model P-97) with 7–10 MΩ resistance and filled with a cesium gluconate solution (135 mM gluconic acid, 135 mM CsOH, 1 mM EGTA, 8 mM MgCl, 0.1 mM $CaCl_2$, 10 mM HEPES, 2 mM Mg-ATP, 0.3 mM Na-GTP, 11 mM biocytin). Voltage-clamp recordings were obtained at +10 mV and −70 mV to record IPSCs and EPSCs, respectively. Analog signals were digitized at 10 kHz with an ITC-18 (InstruTECH) and acquired with IGOR software (Wavemetrics). The rates and amplitudes of IPSCs and EPSCs were analyzed using IGOR software. Immediately after the recordings were made, the slices were fixed in 4% paraformaldehyde (PFA) in 0.1 M sodium phosphate buffer (PB, pH 7.4) overnight and equilibrated in 30% sucrose for several hours before freezing in tissue-freezing medium for long-term storage in a −80°C freezer.

For each GC recording, the ratio of IPSCs to EPSCs was expressed as the postsynaptic (PSC) ratio, obtained by dividing the rate of IPSCs by the rate of EPSCs in each GC. Values for the rate of IPSCs, rate of EPSCs, and PSC ratio for each group were expressed as mean value for the group ± SEM. A Student's *t* test was used to determine whether the mean values for any measure were significantly different between groups.

Optogenetic activation of transplanted GABAergic cells. Between 57 and 98 d after SE, acute brain slices were prepared from TLE mice that received control media injections or transplants of VGAT-ChR2-EYFP-expressing MGE cells in the hilus, as described above. The GABAergic cells in the transplants were optically activated using blue light (460–480 nm) transmitted through a GFP filter and microscopic objective of a fluorescent microscope (Olympus BX51WI), whereas the GCs were voltage-clamped at +10 mV. As a control, recordings were also made in acute brain slices from GCs in naive adult ChR2-EYFP transgenic mice. The light intensity at the level of the hippocampal slices was ~2 mW and the stimulus consisted of a circular area of illumination measuring 0.166 mm^2. The light stimuli consisted of five pulses of 5 ms duration with an interstimulus interval of 200 ms. The pulses were triggered using a Master-8 stimulator (AMP Instruments).

The amplitudes of induced IPSCs were measured using IGOR software. For each GC, the mean amplitude of induced IPSCs was calculated by taking a mean of the amplitudes of all IPSCs induced in response to all the light pulses in a single stimulus across several trials. The induced IPSC amplitude for each group was expressed as the mean value for the group ± SEM.

Thick section analysis of transplants following electrophysiology. Vibratome sections from electrophysiology experiments were stained with rabbit anti-GFP-conjugated with AlexaFluor 488 (Life Technologies) and Texas Red Avidin D (Vector Laboratories) to visualize the transplanted neurons and biocytin-filled GCs. Sections were counterstained with TO-PRO-3 (Life Technologies) and mounted in Prolong Gold with DAPI (Life Technologies). Following staining, the transplants and sites of potential synapses were analyzed by confocal microscopy (Zeiss LSM 510).

Timm stain for analysis of MFS. Timm staining and MFS quantification were performed as described previously with slight modifications (Buckmaster and Dudek, 1997; Buckmaster et al., 2009). Following vibratome sectioning, brain slices were immersed in sodium sulfide solution for 20 min, fixed in 4% PFA for 15 min, cryoprotected in 30% sucrose solution in 0.1 M PB, then stored in an antifreeze solution at −20°C. For Timm staining, the thick slices were cut at 12 μm, mounted onto slides, developed for 35–40 min in Timm developer, counterstained with cresyl violet, dehydrated, cleared in xylene, and mounted in DPX (Sigma-Aldrich).

Graft reconstructions. The extent of dispersion following transplantation was evaluated by reconstructing each graft from immunostained vibratome sections. To compute the volumes of the transplants, we obtained confocal *z*-stack images of the sections. We then charted the locations of $Venus^+$ cells and axonal arborizations onto sections of the mouse brain in the horizontal plane using a digital stereotaxic atlas of the mouse brain (Paxinos and Franklin, 2008). Using ImageJ, we calculated the volume of grafts from confocal images at 100 μm intervals throughout the DG and CA3.

Primary cell culture. To analyze the composition of MGE cells used for transplantation, the MGE progenitors were dissected and dissociated as described above and plated on poly-L-lysine (Sigma-Aldrich)-coated glass coverslips (Fisher Scientific) at a concentration of 1×10^6 cells/ml in serum-free neurobasal medium (Invitrogen) with B27 supplements (Invitrogen), 200 mM glutamine, 25 mM glutamate, and 5000 I.U./ml penicillin and 5000 μg/ml of streptomycin (Cellgro). The cells were cultured up to 14 d in a humidified 37°C incubator with 5% CO_2 and subsequently characterized by immunostaining.

In vitro *immunohistochemical characterization of MGE cells used for transplantation.* MGE cells were grown on coated coverslips as described above, fixed and immunostained to characterize the cell types used for transplantation, based on overlapping expression of VGAT-Venus, in combination with neuropeptides, calcium binding proteins, and other cell-type-specific markers. The immunocytochemical staining was performed on the coverslips using an overnight incubation in primary antibodies at room temperature. The following primary antibodies were used: mouse anti-GFP (1:1000, Life Technologies), rabbit anti-GFP-conjugated with Alexa 488 (1:1000, Life Technologies), rabbit anti-parvalbumin (PV; 1:1000, Millipore), rabbit anti-somatostatin-14 (SOM; 1:1000, Bachem/Peninsula Laboratories), rabbit anti-calbindin (CB; 1:1000, Swant), mouse anti-calretinin (CR; 1:1000, Swant), mouse anti-gephyrin (1:300, Synaptic Systems), and rabbit anti-neuropeptide Y (NPY; Peninsula Laboratories). Detection of primary antibody labeling was performed with the appropriate species-specific secondary antibodies conjugated to AlexaFluor 568 (Life Technologies). Following immunostaining, nuclei were labeled with NeuroTrace 640/660 (1:500, Life Technologies) and the coverslips were mounted with Prolong Gold with DAPI (Life Technologies).

Immunohistochemistry in brain sections. Mice were killed with sodium pentobarbital (Henry Schein, 100 mg/kg, i.p.), and perfused with fixative (4% PFA in 0.1 M PB, pH 7.4). Twelve-micrometer-thick horizontal sections were immunostained to characterize the transplanted cells using the primary and secondary antibodies described above. Nuclei were stained with NeuroTrace 640/660 (1:500, Life Technologies) or

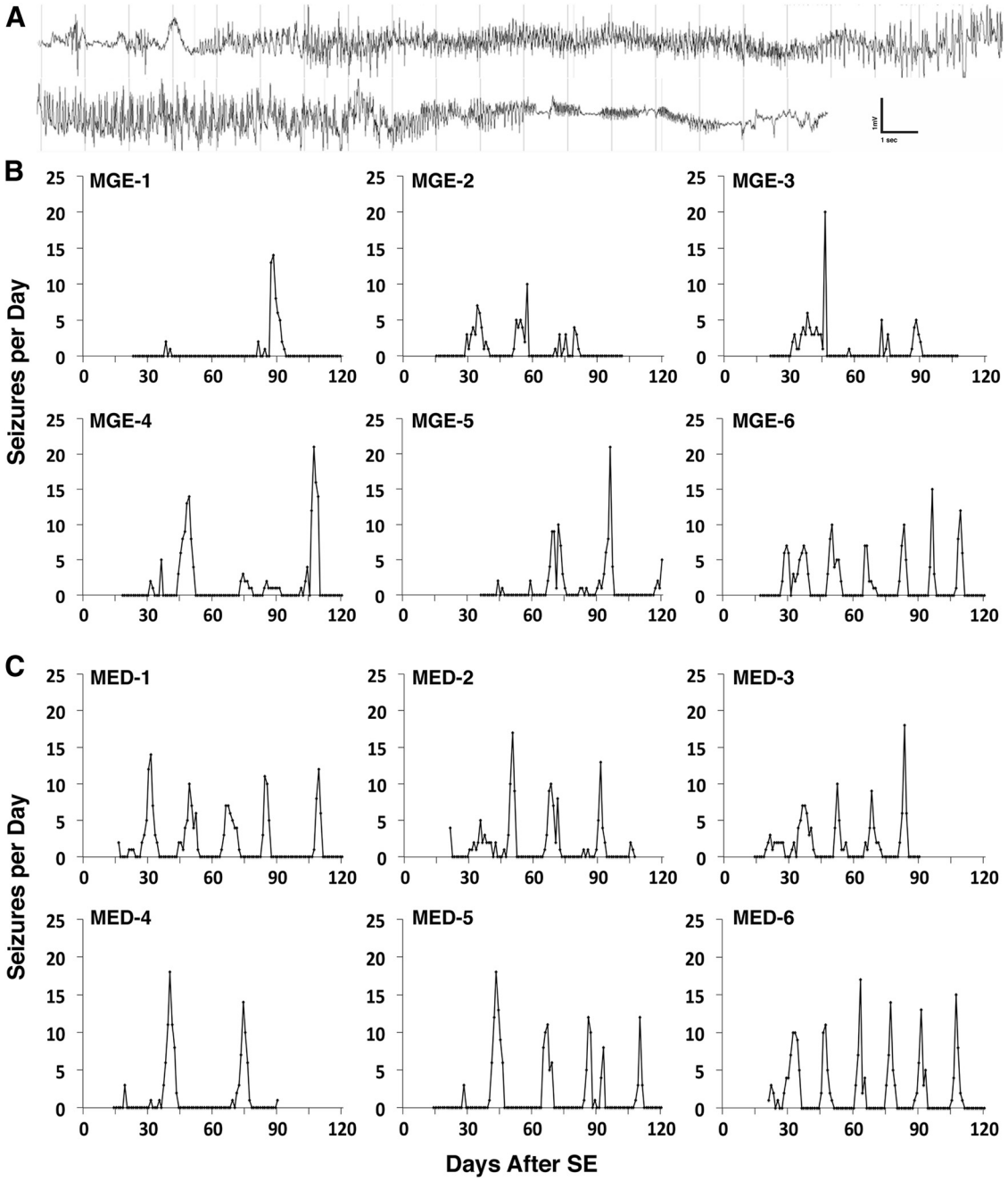

Figure 1. Comparative analysis of patterns of clustered seizure activity in experimental mice with TLE that received MGE grafts versus controls. Forty-two TLE mice were monitored with V-EEG recordings and of these, 15 mice had continuous monitoring from ~21 d after SE to ~90–100 d after SE. These mice were selected for further analyses to examine disease-modifying effects of the transplants. Approximately 14 d after inducing SE, a group of TLE mice received stereotaxic injections of E13.5 MGE cells into the hilus of the DG and controls received stereotaxic injections of cell-free media into the hilus. ***A***, Representative EEG recording of a seizure in a TLE mouse that received bilateral MGE cell transplants in the hilus. ***B***, Graphs showing the frequency of seizures/day over time in mice with MGE transplants into the hilus. Five of six mice showed fewer daily seizures. ***C***, Mice with media injections into the hilus typically displayed regular clusters of seizures lasting 5–7 d with intercluster intervals of 5–10 d.

TO-PRO-3 (1:5000, Life Technologies) for Meta confocal microscopy (Zeiss LSM 510) or mounted with Prolong Gold with DAPI (Life Technologies) for fluorescent microscopy (Zeiss Axiovert 200 M).

Quantification of gephyrin puncta. Brain sections, 12-μm-thick and immunohistochemically stained for GFP and gephyrin, were imaged with a Zeiss LSM 510 Meta confocal microscope to generate 3-D *z*-stack images with a slice interval set at 0.3 μm. Lengths of transplanted axons from these images were reconstructed in Adobe Photoshop by tracing axons and gephyrin puncta using a drawing tablet (Wacom Bamboo Capture). These reconstructions were then analyzed to quantify sites of apposition between gephyrin puncta and en passant and terminal synaptic boutons. Only puncta within distances of 0.3 μm or less of the synaptic boutons were quantified. The proximity of all gephyrin puncta to presynaptic boutons was confirmed in confocal *z*-stack images with Zeiss Zen software.

Results

MGE transplants are associated with reductions in seizure frequency and total seizure duration

We recorded EEGs from a total of 42 mice with transplants and 18 mice with media injections. For seizure analyses, we only in-

cluded mice with bilateral DG transplants that had continuous V-EEG recordings from 40 d after SE to 90–100 d after SE (Fig. 1). These subjects included the following: nine controls injected with media, six mice with bilateral MGE transplants into the hilus, and four mice with MGE cells injected into the LEC. The controls generally had seizure patterns that were characteristic of the pilocarpine model, with seizures occurring in clusters lasting 5–7 d (range, 3–10 d) interspersed with seizure-free periods of variable lengths, typically from ~5–10 d (Fig. 1*C*). Of six mice with bilateral MGE cell transplants in the hilus, five showed suppression (Fig. 1*B*). In the one mouse that did not show suppression, we verified that there were surviving bilateral MGE cell transplants. During seizures, all of the experimental mice also exhibited behavioral changes characteristic of SRS including immobility, staring, limb clonus, and loss of postural control (data not shown).

To further investigate the disease modifying effects of the transplants, we calculated the seizure frequency per group. TLE mice with transplants in the hilus had significantly fewer seizures than those injected with media for the entire 40–100 d V-EEG period of recording (ANOVA, $p = 0.008$). During this period, the group of four mice with MGE transplants in the LEC showed the highest average number of seizures (159 ± 19 *SEM*), whereas control TLE mice showed an intermediate number of seizures (123 ± 4 SEM), and the group of TLE mice with hilar MGE transplants had the fewest seizures (78 ± 8 SEM). Comparing the group of media-injected control mice with the group receiving hilar transplants revealed on overall reduction of ~37%.

To further examine the time course for transplant-mediated seizure suppression, we evaluated the number of seizures for the transplant group versus the media control group during three contiguous 20 d intervals from 40–60, 61–80, and 81–100 d after SE (Fig. 2*A*). The length of these intervals was selected to compare early, mid, and late effects of transplanting fetal GABAergic interneurons on SRS. During the interval from 40–60 d after SE, corresponding to 26–46 d after transplantation, we found no significant differences in the average number of seizures per group (repeated-measures ANOVA, $p = 0.220$). Notably however, 61–80 d after SE, corresponding to 47–67 d after transplantation, the MGE transplant group had significantly fewer seizures on average (repeated-measures ANOVA, $p =$

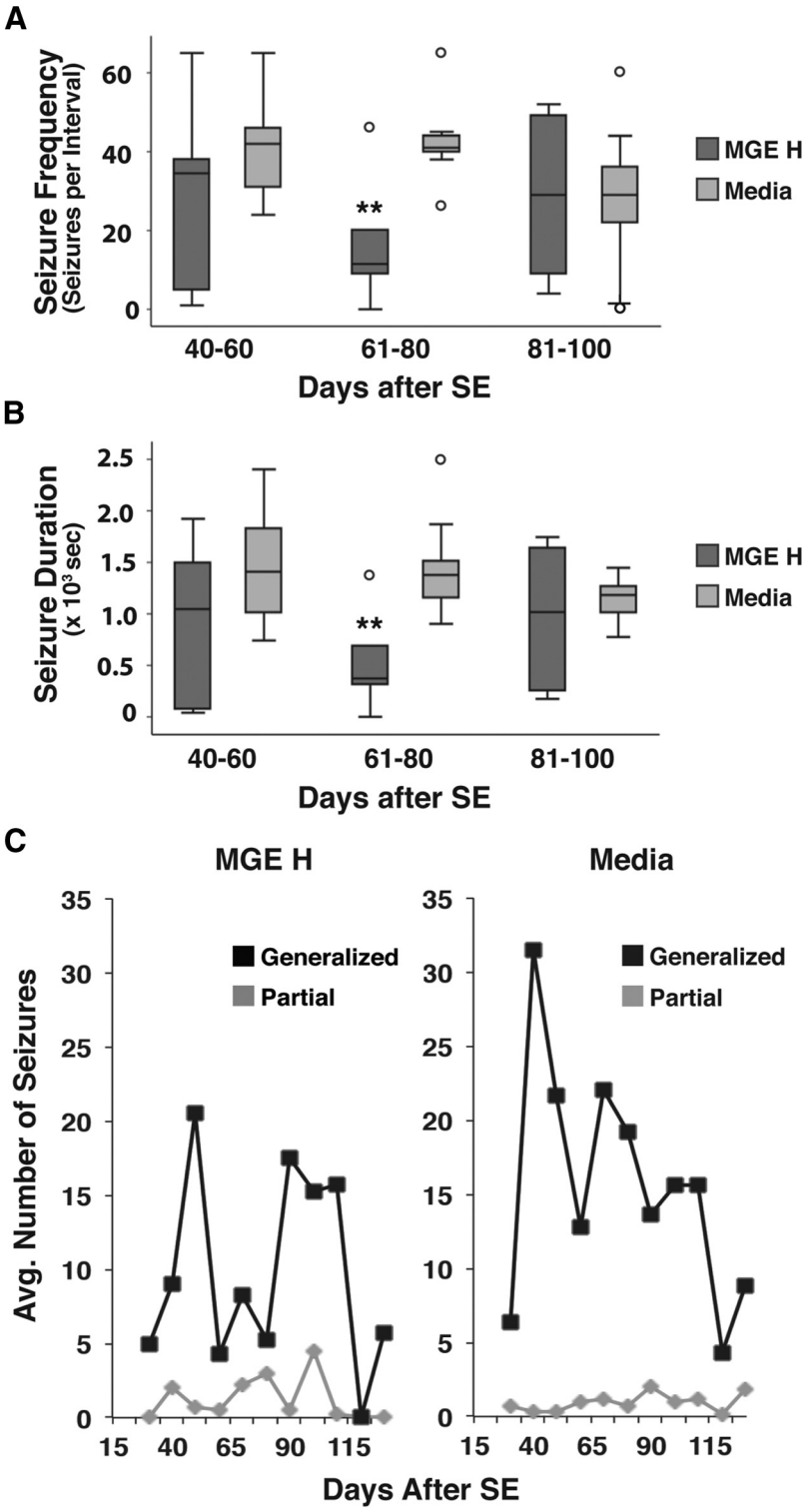

Figure 2. Quantitative analyses of seizure severity in TLE mice. ***A***, TLE mice with MGE transplants into the hilus ($n = 6$) showed significantly fewer seizures during the 61–80 d interval, compared with TLE mice with media injections into the hilus ($n = 9$; $^{**}p = 0.002$). ***B***, The total time spent having seizures was significantly less in TLE mice with MGE transplants into the hilus ($n = 6$) during the 61–80 d interval ($^{**}p = 0.003$). In the box and whisker plots, the boxes represent the range between first and third quartiles. The line within the box is the median. The top whisker extends to the largest data point less than or equal to the third quartile plus 1.5× interquartile range. The lower whisker extends to the smallest data point greater than or equal to the first quartile minus 1.5× interquartile range. Outliers are data points beyond the whiskers. ***C***, Additional analyses were conducted using the Racine behavioral scale to determine whether the mice showed differences in partial (stages 1–2) or generalized seizures (stages 3–6). These behavioral analyses were done for the entire period of recordings and showed that TLE mice with hilar MGE transplants (MGE H) had fewer generalized seizures with predominantly milder, focal seizures compared with controls that had media injections (Media; Student's *t* test, $p = 0.0001$).

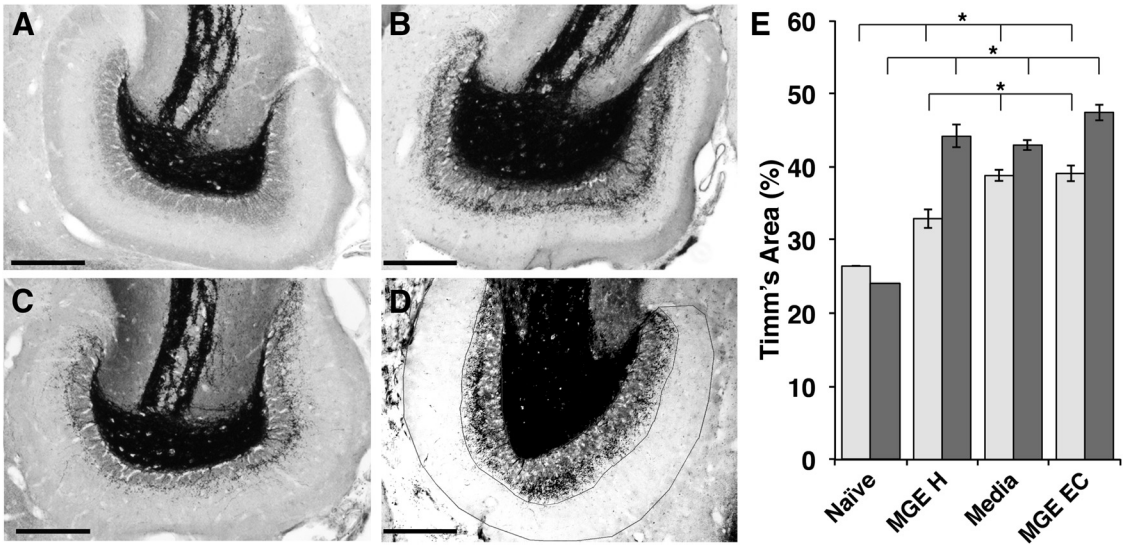

Figure 3. The area of Timm-positive staining in the DG was reduced in TLE mice receiving hilar transplants of MGE-derived GABAergic interneurons. ***A***, Photomicrograph showing the DG from a naive control mouse. In naive mice, Timm staining does not extend into the inner molecular layer of the DG, indicating no MFS. ***B***, Ninety to 100 d after SE, TLE mice with media injections showed robust MFS invading the inner molecular layer. ***C***, Mice with MGE transplants in the hilus showed suppression of MFS in the inner molecular layer of the DG. The GCL was stained for cresyl violet in blue (***A–C***). Quantification method is shown in ***D***. ***E***, All TLE mice had significantly more Timm-positive area in the molecular layer of the DG in sections from the dorsal hippocampus (light gray bars) compared with naive mice that had no pilocarpine or surgery treatment (ANOVA, $p < 0.0001$). Timm staining in the inner molecular layer in the dorsal hippocampus of mice with MGE cell transplants ($n = 8$) compared with mice with media injections ($n = 3$; ANOVA, $p < 0.0001$). Mice with MGE cell transplants into the LEC ($n = 3$) were equivalent to mice with media injections. All TLE mice had significantly more Timm-positive area in the molecular layer of the DG in sections from the ventral hippocampus (dark gray bars) in comparison to naive mice ($n = 3$; ANOVA, $p < 0.0001$). Scale bars: *A–D*, 200 μm.

0.0018). No significant differences were found in the third interval, from 81–100 d after SE (repeated-measures ANOVA, $p = 0.950$). Additionally, we observed a significant effect of the MGE transplants on the duration of time TLE mice spent in seizures in the 61–80 d interval (Fig. 2*B*; repeated-measures ANOVA, $p = 0.0031$). Furthermore, the TLE mice receiving MGE transplants into the hilus had significantly fewer generalized (stages 3–6) seizures, compared with controls with only media injections (Fig. 2*C*; Student's *t* test, $p = 0.0001$). Thus, we found a significant effect of GABAergic interneuron grafts on three different measures of disease outcome: seizure frequency, duration, and severity. These effects were not apparent immediately, requiring several weeks after transplantation for the effects to be detected. Given the relatively small group sizes (6–9 mice per group) and the variability in the cluster patterns, intercluster intervals, and severity of TLE in different mice, the effects of the hilar transplants on seizure suppression were remarkably robust. Notably, we found that the disease-modifying effects of MGE grafts did not persist for the entire period of the recordings, since significant suppression was not observed in the last period of the V-EEG recordings from 81–100 d after SE.

To determine whether the upsurge in seizures during the later periods of recording was due to the size of the grafts, we evaluated whether greater suppression was correlated with larger areas of graft innervation. On average, cells and processes from the transplanted GABAergic interneurons occupied ~30–50% of the total DG (mean transplant size = 1.3×10^8 μm^3, SEM = 3.4×10^7 μm^3). The mice with larger transplants tended to exhibit reduced seizure frequencies, however, this effect did not reach statistical significance.

Based on the findings that the TLE mice receiving transplants of MGE-derived GABAergic progenitors showed fewer and milder seizures, we next examined whether these mice also exhibited reduced MFS, a neuroplastic phenomenon linked to GC hyperexcitability and SRS (Tauck and Nadler, 1985; Buckmaster and Dudek, 1997; Nadler, 2003; Walter et al., 2007; Scharfman and Pierce, 2012).

Compared with naive mice (Fig. 3*A*), MFS in the molecular layer of the DG in TLE mice (Fig. 3*B*) was greater at dorsal and ventral levels of the hippocampus (Fig. 3*E*). However, mice with hilar MGE transplants (Fig. 3*C*) showed significantly reduced MFS in the vicinity of the MGE transplants in the dorsal hippocampus, compared with TLE mice receiving media or LEC transplants (Fig. 3*E*; ANOVA, $p < 0.0001$). Although further studies are needed to determine the underlying mechanisms for this effect, one intriguing possibility is that the formation of reciprocal synaptic connections between the transplanted GABAergic interneurons and dentate GCs may reduce MFS into other regions.

Transplants contain subtypes of GABAergic interneurons

The fetal tissue for transplantation was derived from the MGE, a region that gives rise to multiple subtypes of forebrain GABAergic interneurons. To identify whether particular functional subtypes of GABAergic interneurons were linked to seizure suppression, we compared the phenotypes of MGE cells after transplantation with the composition of MGE cell cultures maintained *in vitro* for 7–21 d. Dual immunofluorescent labeling of MGE-derived Venus-expressing cells was combined pairwise with neurochemical markers to distinguish different interneuron subtypes. These analyses in TLE mice with hilar transplants showed that the grafts contained multiple functional subtypes of interneurons. Approximately 15% of grafted cells differentiated into PV-expressing (PV^+) interneurons (15 ± 5%; $n = 6$ mice; 2565 cells); 25% were SOM-expressing (SOM^+) interneurons (25 ± 9%; $n = 7$ mice; 2528 cells); 36% were NPY-expressing (NPY^+) interneurons (36 ± 12%; $n = 4$ mice; 1279 cells); and 42% were CB-expressing (CB^+) interneurons (42 ± 6%; $n = 4$ mice; 208 cells). CR-expressing (CR^+) cells were only present in very low numbers ($n = 2$ mice; 754 cells; Fig. 4*A–D*, *G*).

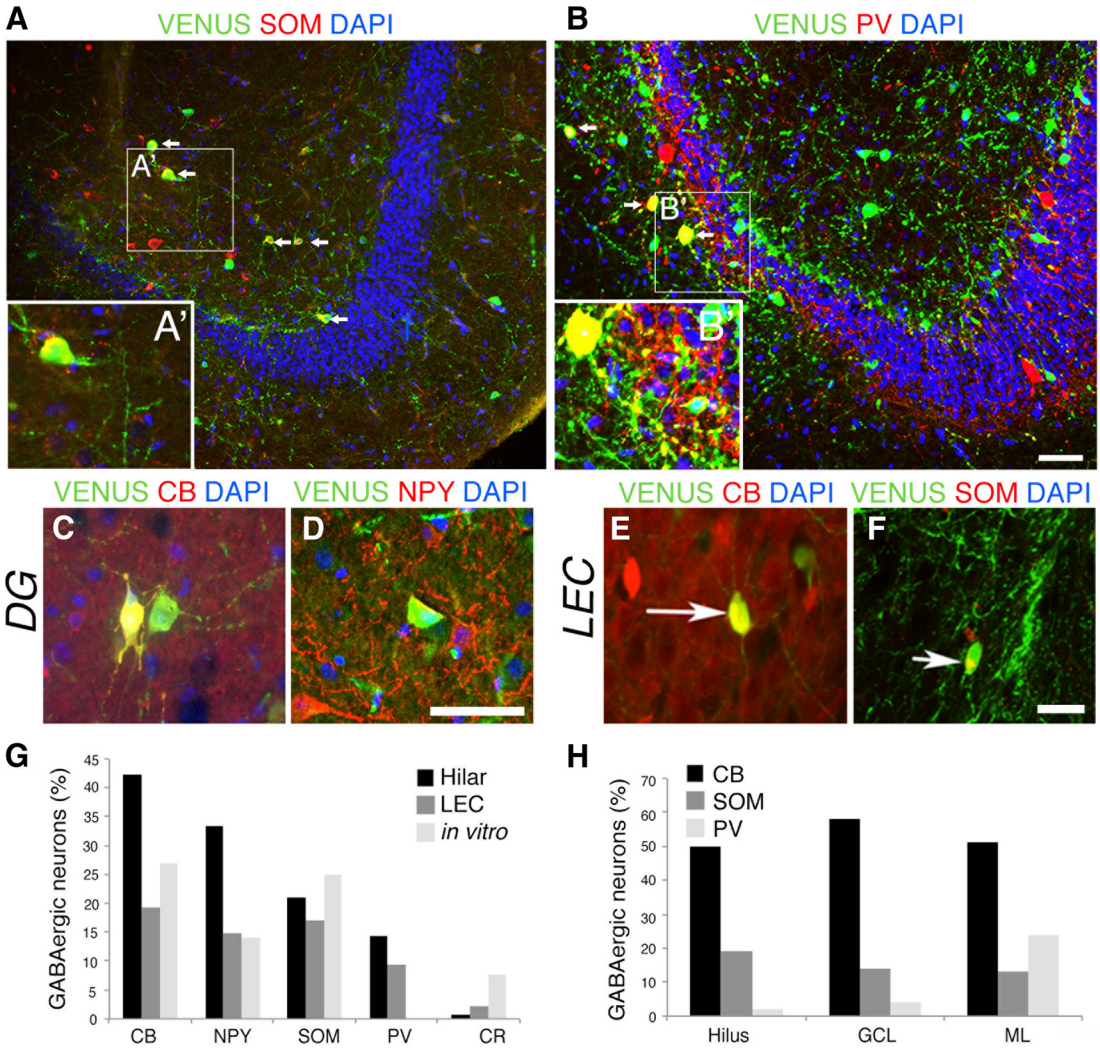

Figure 4. MGE-derived progenitors engrafted into the DG or LEC differentiated into multiple subtypes of GABAergic interneurons that coexpressed neuropeptides and calcium binding proteins. ***A***, MGE-derived GABAergic interneurons expressing SOM were identified throughout the DG. ***A′***, Highly-magnified view of SOM $^+$ GABAergic interneuron within the hilus. ***B***, MGE-derived GABAergic interneurons expressing PV were commonly found in the molecular layer (ML) and GCL. ***B′*** Highly-magnified view of VGAT-Venus/PV $^+$ GABAergic interneuron within a transplant that formed axonal and dendritic arborizations within the GCL. Endogenous PV $^+$ interneurons formed dense axonal endings as well. ***C–D***, MGE-derived interneurons also expressed CB and NPY. ***E–F***, Subsets of the MGE-derived progenitors engrafted into the LEC differentiated primarily into CB $^+$, NPY $^+$, or SOM $^+$ GABAergic interneurons and rarely into PV $^+$ or CR $^+$ subtypes. ***G***, Quantitative analyses showed that the most prevalent subtypes of GABAergic interneurons in grafts made into the hilus of the DG were CB $^+$ (>40%), NPY $^+$ (33%) or SOM $^+$ (~20%; $n = 7$ mice, 8707 cells). These populations likely represent partially overlapping subsets of GABAergic interneurons. Similar, but lower percentages of these phenotypic markers were found in transplants made into the LEC ($n =$ 3 mice, 813 cells), and in MGE cells that matured *in vitro* ($n = 3$ separate primary MGE cell cultures, 5735 cells). ***H***, Distinct differences were found in the distributions of different subtypes of MGE-derived GABAergic interneurons within the layers of the DG. Populations of SOM $^+$ and PV $^+$ interneurons were significantly enriched in the GCL and ML relative to the hilus (PV $^+$ interneurons, Student's t test, $p < 0.001$; SOM $^+$ interneurons, Student's t test, $p < 0.01$), but there were no significant differences in the laminar distributions of CB $^+$ interneurons in the different layers of the DG. Arrows in ***A***, ***B***, ***E***, ***F***, indicate VGAT-Venus $^+$ interneurons coexpressing neuropeptides or calcium binding proteins. Scale bars: ***A–D***, 50 μm; ***E***, ***F***, 25 μm.

We also observed marked differences in the distributions of the different GABAergic interneuron subtypes within the DG (Fig. 4*H*). PV $^+$ neurons were found throughout the DG; however, they were enriched in the GC and molecular layers. Similarly, transplant derived SOM $^+$ neurons resembling previously described hilar GABAergic interneurons (Freund and Buzsáki, 1996) were found throughout the DG, however proportionally more were in the GC and molecular layers, compared with the hilus of the dentate gyrus (Student's t test, $p = 0.003$). In contrast, CB $^+$ interneurons were evenly distributed throughout these layers of the dentate gyrus. These results suggest that the GC and molecular layers may provide enhanced survival conditions for the transplanted PV $^+$ and SOM $^+$ interneurons.

To further examine this question, we determined whether the initial composition of the transplants was similar, by comparing the composition of the transplants with MGE cells differentiated for brief periods *in vitro*. After 1–2 weeks, the composition of the MGE cultures was ~27% CB $^+$ interneurons (27 ± 7%; $n = 3$ cultures; 1908 cells), 25% SOM $^+$ interneurons (25 ± 3%; $n = 3$ cultures; 1160 cells), and <10% of the remaining subtypes of CR $^+$ (8 ± 3%; $n = 3$ cultures; 934 cells), and NPY $^+$ interneurons (8 ± 4%; $n = 3$ cultures; 245 cells). We also found a small percentage of platelet-derived growth factor receptor α-positive (PDGFRα^+) cells (6 ± 5%, $n = 3$ cultures), consistent with either oligodendrocyte progenitors or rare subsets of neurons from the MGE that express this receptor after maturation (Nait Oumesmar et al., 1997; Woodruff et al., 2001). Curiously, we rarely detected PV $^+$ interneurons in these cultures.

We also characterized the subtype composition of MGE-derived Venus-expressing cells transplanted into the LEC (Fig. 4

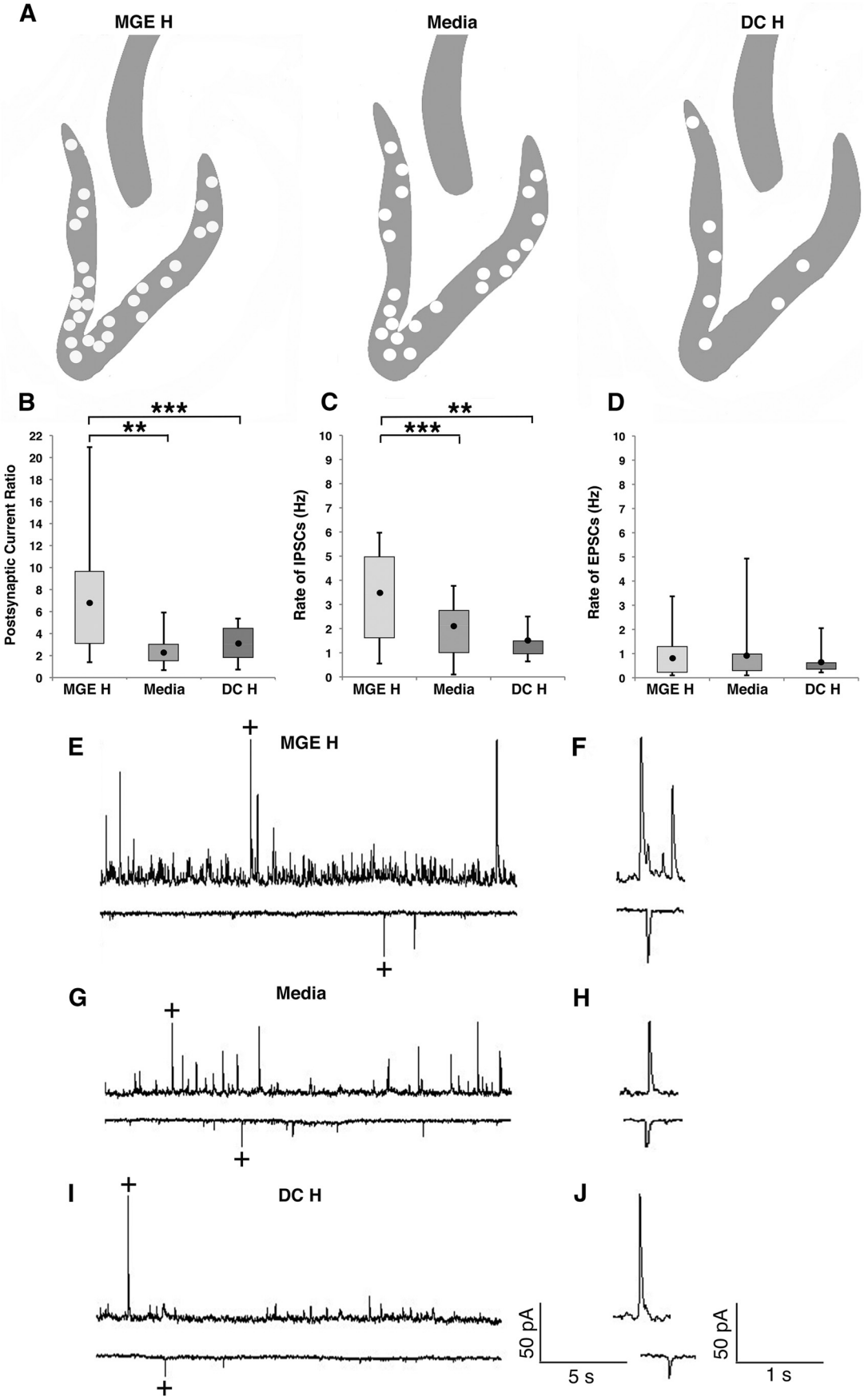

Figure 5. Increased rates of IPSCs in granule cells recorded from TLE mice receiving MGE cell grafts. Whole-cell patch-clamp recordings were performed in a total of 77 GCs. ***A***, Schematic drawings of the DG show the locations of the different GCs recorded from three groups of mice. In mice with MGE transplants (MGE H), morphological reconstructions were obtained for 26 of 34 GCs. In mice with media injections (Media), morphological reconstructions were obtained for 22 of 30 GCs. In mice with dead-cell injections (DC H), 7 of 13 recorded GCs were (*Figure legend continues.*)

E–G) Within these grafts, the composition was similar to the dentate grafts: 19% were CB^+ (19 ± 11%; $n = 4$ mice; 125 cells), 17% were SOM^+ (17 ± 6%; $n = 6$ mice; 228 cells), 15% were NPY^+ (15 ± 8%; $n = 3$ mice; 128 cells), 10% were PV^+ (10 ± 8%; $n = 5$ mice; 199 cells), and just 2% were CR^+ ($n = 3$ mice; 133 cells).

These results show that the transplants in the DG are heterogeneous and suggest that one or multiple subtypes of interneurons could account for the observed reductions in SRS. We also noted that the subtypes of GABAergic interneurons tended to disperse from the hilus into the GCL and molecular layers. Thus, different types of inhibitory neurons in the transplants could influence dentate circuit function in a location-specific manner within the DG and to begin to address this question, we compared postsynaptic currents in GCs from mice with hilus transplants or control injections of media or dead cells.

Hippocampal slices from TLE mice with MGE transplants show increased synaptic inhibition onto granule cells

To determine whether transplanted GABAergic interneurons increased synaptic inhibition on GCs, we recorded spontaneous IPSCs and EPSCs in GCs from a total of 77 cells in 22 mice, including 30 GCs from controls injected with media, 13 GCs from controls injected with dead cells, and 34 GCs from mice with interneuron transplants surviving 90–130 d (Fig. 5*A*). The PSC ratio was used to assess synaptic integration. We found that control mice injected with media had a mean PSC ratio of 2.73 ± 0.27, and similarly, mice with dead cell transplants into the hilus had a mean PSC ratio of 3.04 ± 0.44. In contrast, the GCs from mice with MGE transplants in the hilus had at least two times larger PSC ratios (mean PSC ratio 6.9 ± 0.94). These findings show a dramatic and statistically significant increase (Student's *t* test, $p = 0.0001$) in IPSCs in mice with MGE transplants (Fig. 5*B*). Moreover, we found that the rate of IPSCs was significantly higher in slices containing MGE transplants (3.47 ± 0.41) compared with controls with media injections (2.12 ± 0.32, Student's *t* test, $p = 0.010$) or dead cells (1.51 ± 0.26, Student's *t* test, $p = 0.006$; Fig. 5*C*). No significant differences were found in the rate of EPSCs (Fig. 5*D*). Examples of individual recordings show that GCs from mice with hilar MGE transplants exhibited many more spontaneous IPSCs (Fig. 5*E*) compared with GCs in controls (Fig. 5*G*,*I*). The mean amplitude of IPSCs in mice with MGE transplants was 15.1 ± 0.90 pA compared with 15.6 ± 0.98 pA in mice with media injections (Student's *t* test, $p = 0.68$) and 12.0 ± 0.72 pA (Student's *t* test, $p = 0.05$) in mice with dead-cell injections. Similar to the trend for mean IPSC amplitude, the mean EPSC amplitude was almost equal in mice with MGE transplants (7.23 ± 0.45 pA) and mice with media injections (7.27 ± 0.31 pA; Student's *t* test, $p = 0.94$) but the EPSC amplitude in mice with dead cell injections was 6.1 ± 0.38 pA (Student's *t* test, $p = 0.14$; Fig. 5*F–J*). These experiments suggest that the transplanted GABAergic interneurons were responsible for the observed increase in IPSCs in GCs.

Transplanted GABAergic interneurons develop inhibitory synaptic networks with granule cells

To further investigate inhibitory synaptic connections between GCs and VGAT-Venus or VGAT-ChR2-EYFP transplanted cells, we performed high-resolution confocal microscopic imaging analyses in sections containing biocytin filled GCs in the vicinity of large transplants (Fig. 6). These experiments confirmed dense networks of synaptic contacts formed by the transplanted GABAergic interneurons onto GC dendritic shafts, somas, and axon initial segments (Fig. 6*A–C′*). To further verify the presence of functional inhibitory synapses, additional brain sections containing transplanted MGE cells and their axons were immunostained for the postsynaptic scaffolding protein gephyrin and quantitative analyses were carried out. Approximately 60% of the axonal boutons of the transplanted MGE-derived GABAergic interneurons were associated with multiple postsynaptic clusters of gephyrin, as confirmed by analyses of *z*-stacks. On average, axons had 2.166 gephyrin puncta (SEM ± 0.33 puncta) per 10 μm of axon length. The gephyrin puncta were on average 0.66 μm (SEM ± 0.04 μm) in diameter. Further confirming a possible synaptic mechanism for seizure suppression, these immunohistochemical studies show that MGE-derived inhibitory neurons in TLE mice form extensive inhibitory synaptic connections with hippocampal GCs.

Optogenetic activation of transplanted GABAergic interneurons expressing channelrhodopsin generates strong IPSCs in granule cells

Having determined that the transplanted GABAergic neurons established extensive synaptic contacts with GCs, we next sought to determine whether these new synapses were functional. To address this question, we recorded from GCs in six TLE mice that had received grafts consisting of ChR2-EYFP-expressing GABAergic progenitors at 6–12 weeks after transplantation. We first verified in brain slices from adult VGAT-ChR2-EYFP transgenic mice that light-mediated activation of endogenous hippocampal GABAergic interneurons induced strong IPSCs in dentate GCs (mean amplitude 217.38 ± 39.27 pA, $n = 15$ cells; Fig. 7*A*,*B*). We next recorded from GCs in acute brain slices from experimental mice with TLE that had received transplants into the hilus of embryonic VGAT-ChR2-$EYFP^+$ cells (Fig. 7*C*,*D*). Similar to slice experiments in which we optogenetically stimulated the endogenous ChR2-EYFP-expressing interneurons with blue light, depolarizing transplanted GABAergic interneurons with light also induced strong IPSCs in GCs (mean amplitude 80.32 ± 18.19 pA, $n = 21$ cells). In total, we recorded from 23 GCs ($n = 6$ mice) in slices containing transplanted GABAergic neurons and observed light-induced IPSCs in 21 of these. Dual staining for biocytin and EYFP confirmed the presence of transplanted interneurons in the slices. Additionally, the putative synaptic contacts formed between the transplanted interneurons and biocytin-filled GCs were visualized using high-resolution confocal imaging. As a control, we tested whether light had nonspecific effects, in the absence of ChR2-expressing transplants. We conducted these control recordings in 22 GCs from slices lacking transplanted cells. As predicted, none of the GCs in these experiments showed a response to light. These immunohistochemical and electrophysiological experiments support and extend the V-EEG findings by showing that engrafted GABAergic interneu-

←

(*Figure legend continued.*) morphologically identified. ***B–D***, Statistical comparisons of rates of postsynaptic currents showed a significantly higher rate of IPSCs in the mice with MGE transplants, compared with controls. The bottom whiskers of the graph denote the minimum values and the top whiskers denote maximum values. The boxes represent the first and third quartiles. The dots indicate the mean value for the groups. ***E***, Representative recordings are shown from mice with MGE transplants in the hilus; ***G***, mice with media injections; and ***I***, mice with dead cell injections. Upward deflections represent IPSCs and downward deflections represent EPSCs. ***F***, ***H***, ***J***, PSCs marked with cross in ***E***, ***G***, and ***I***, respectively; ** $p < 0.01$, *** $p < 0.05$.

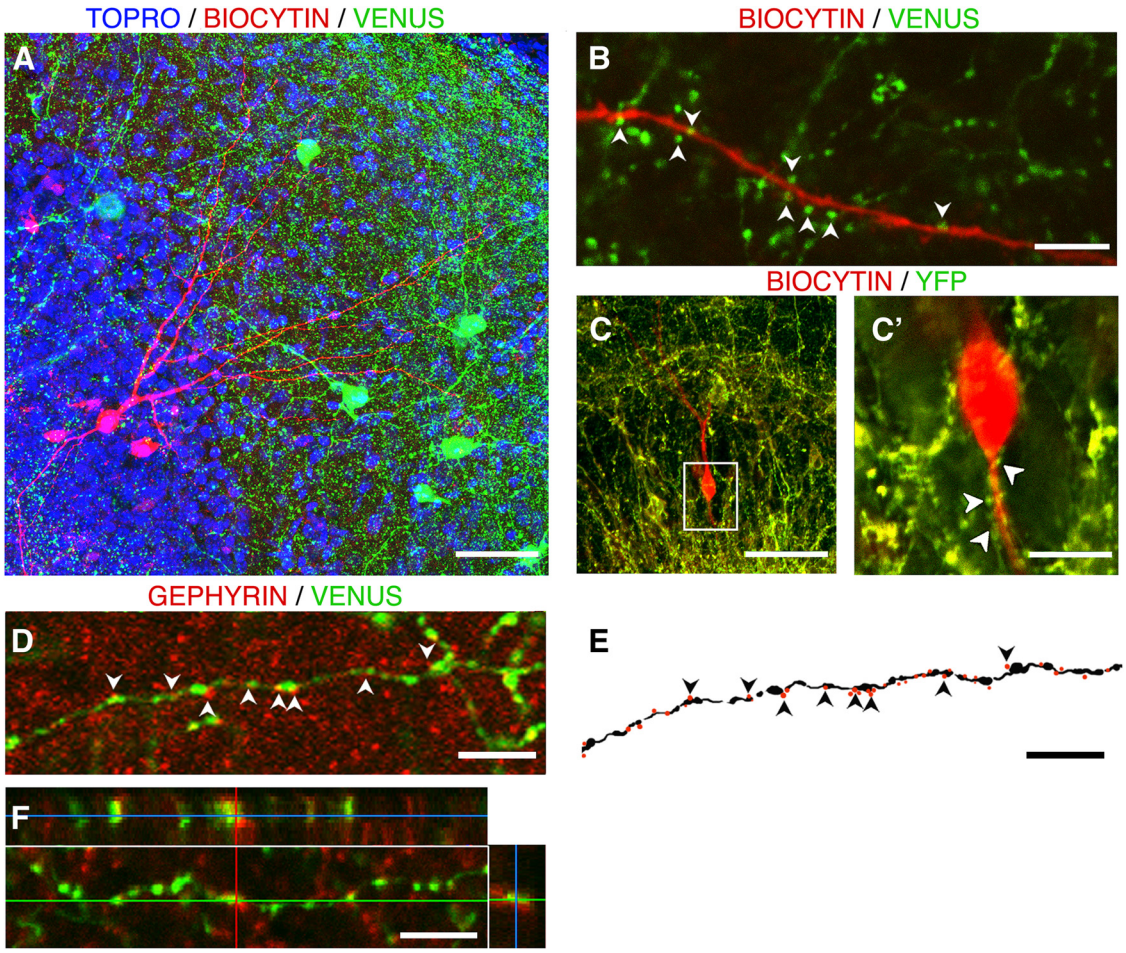

Figure 6. Transplanted GABAergic interneurons establish extensive inhibitory synaptic networks with granule cells in the dentate gyrus of TLE mice. ***A***, Representative section showing the locations of transplanted MGE-derived GABAergic interneurons expressing Venus fluorescent protein (green) in the GC and molecular layers of the DG. The axonal processes of the transplanted cells are shown surrounding the dendrites of biocytin-filled GCs (red) in the inner and outer molecular layers of the DG. ***B***, Axonal boutons of Venus-labeled GABAergic interneurons are shown contacting the dendrite of a biocytin-filled GC. ***C***, Axonal arbors of transplanted ChR2-EYFP-expressing GABAergic interneurons form putative synapses onto a biocytin-filled GC that showed pronounced IPSCs in response to optogenetic stimuli. ***C′***, Boxed region from ***C***, showing sites of putative synapses onto the soma, dendrites, and axon initial segment of the GC shown in ***C***. ***D***, Representative axon from a transplanted GABAergic interneuron with synaptic varicosities in close apposition to postsynaptic gephyrin puncta. ***E***, Reconstruction of the same axon as ***D*** for quantification of gephyrin puncta. ***F***, Confocal image from a *z*-stack showing representative synaptic contacts onto GCs containing postsynaptic gephyrin puncta. One of these sites is marked by crosshairs showing close apposition in *x*-, *y*-, and *z*-axes between a presynaptic Venus $^+$ GABAergic axon and a large cluster of postsynaptic gephyrin. Scale bars: ***A***, 50 μm; ***B***, 2.5 μm; ***C***, 50 μm; ***C′***, 15 μm; ***D***–***F***, 7.5 μm. Arrowheads in ***B***, ***C′***, ***D***, and ***E*** indicate putative synaptic connections.

rons establish active and functional inhibitory synapses onto GC cell bodies, dendrites, and axons.

Discussion

In patients with severe MTLE and intractable seizures, reorganization of the DG may include loss of hilar interneurons, axonal sprouting, altered GC densities, and increased excitability (Margerison and Corsellis, 1966; Houser, 1990; de Lanerolle et al., 2003, 2012; Swartz et al., 2006). Managing seizures in patients with severe MTLE is often challenging, possibly due to these diverse neuroplastic changes. GABAergic interneuron-based cell therapies have gained traction in recent years, supported by an extensive series of studies showing that engraftment of GABAergic progenitors into the cerebral cortex or hippocampus resulted in seizure suppression in various experimental models of epilepsy (Tyson and Anderson, 2014).

To understand seizure suppression at a more mechanistic level, we examined the time course for seizure suppression following MGE transplantation into the DG in the mouse pilocarpine model of TLE. Through continuous V-EEG recordings for 60 or more days, we found 35% suppression of SRS in mice with MGE-derived GABAergic cell grafts in the DG, compared with control injections and associated reductions in seizure duration and seizure severity. Our electrophysiological experiments further showed that the engrafted interneurons were capable of eliciting strong postsynaptic inhibitory currents in GCs suggesting that when the transplanted cells integrate into the neural circuits of the DG, they increase inhibition of dentate GCs. These findings indicate that transplanting immature GABAergic interneurons into the hippocampus of adult mice with TLE reduces seizures and other pathophysiological features of MTLE by altering hippocampal circuitry.

Continuous EEG monitoring in rodents with pilocarpine-induced TLE has shown that SRS occur in clusters over 3–7 d with 1–2 week or longer intercluster intervals (Curia et al., 2008; Mazzuferi et al., 2012). By extending the period of continuous EEG analyses for 60 d, we found that effects of the transplants on seizures did not become evident until ~6 weeks after transplantation, corresponding to the period between 61–80 d after SE.

These results suggest that the transplanted cells may take a month or longer to synaptically integrate. The observed reductions in SRS were highly significant, but not permanent, as the effects did not extend beyond 80 d after SE. These findings support and extend prior studies demonstrating seizure suppression for shorter periods following MGE transplants (Hunt et al., 2013). Given the clustered and periodic nature of seizures in the pilocarpine model and seizure-free intervals of 1–2 weeks, studies that rely on short-term EEG recordings or intermittent observations of behavioral seizures may have overestimated the efficacy of MGE grafts (Baraban et al., 2009; Calcagnotto et al., 2010b; Hunt et al., 2013).

Although the underlying mechanisms causing the observed rebound in seizures in the later periods of observation are not well understood, we verified by optogenetic stimulation that the engrafted cells were still capable of inducing strong hyperpolarizing postsynaptic currents in GCs 57–98 d after SE. The observed rebound in seizures was also unlikely to be due to loss of the transplanted cells, as we verified the presence of the transplants following EEG recordings. One possibility warranting further investigation is that the transplanted interneurons might lose their capacity to establish inhibitory synapses with new GCs born after SE. Examining synaptic connectivity between the transplanted interneurons and GCs born at different times after SE could help resolve this issue and further define temporal constraints on transplant-mediated seizure suppression.

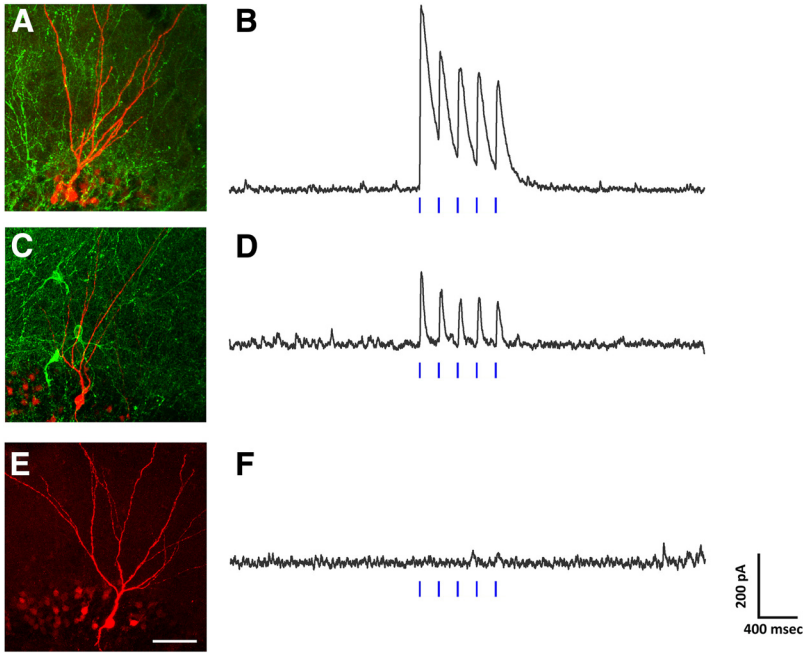

Figure 7. Strong optogenetically induced postsynaptic responses in granule cells demonstrate innervation by transplanted ChR2-expressing GABAergic interneurons. ***A***, Biocytin-filled GC (red) from a VGAT-ChR2-EYFP transgenic mouse receiving GABAergic inputs from endogenous interneurons (green). ***B***, Electrophysiological recording from this neuron showing IPSCs induced by brief optogenetic stimuli (vertical blue bars). ***C***, Biocytin-filled GC (red) in a TLE mouse surrounded by transplanted MGE-derived ChR2-EYFP-expressing GABAergic interneurons and their axonal arbors (green). ***D***, Electrophysiological recording from the GC shown in C, showing strong IPSCs induced by light pulses (vertical blue bars). ***E***, Biocytin-filled GC from the same mouse as in C, which was located at a distance from the region innervated by transplanted ChR2-EYFP-expressing GABAergic interneurons. ***F***, Optogenetic stimuli failed to induce electrophysiological responses in GCs distant from the transplants and an example is shown in ***E***. Recordings were performed 6–12 weeks after transplantation. Vertical blue bars indicate five pulses of 5 ms each of blue light; interstimulus interval equals 200 ms. IPSCs were recorded by voltage-clamping GCs at +10 mV. Scale bars: ***A***, ***C***, ***E***, 50 μm. Bottom, Right, Scale for electrophysiological recordings for ***B***, ***D***, and ***F***.

Our findings showing significant reductions in SRS (35–50%) are somewhat lower than what has been reported previously (Calcagnotto et al., 2010a,b; Waldau et al., 2010; Hunt et al., 2013), and additional studies will be needed to evaluate methodological differences including: seizure models, disease stage at the time of transplant, methods for seizure detection, transplantation sites, cell type composition of the grafts, maturation stage of fetal cells, and the extent to which engrafted cells innervate GCs and/or pyramidal neurons. Our findings provide an accurate assessment of MGE transplant effects on seizures in the pilocarpine model of TLE by documenting seizure incidence, duration, and severity using round-the-clock recording for a 60 d period (in some cases much longer) during the chronic phases of the disease. However, one key difference between our study and prior work concerns the locations of the transplants. We made bilateral injections of 100,000 freshly dissociated fetal MGE cells into the hilus at mid-levels of the DG and the transplanted cells mainly innervated the DG. In contrast, different injection sites including CA3-CA1 and/or multiple injection sites within the hippocampus may result in very different patterns of innervation of different hippocampal neurons, possibly resulting in more complete seizure suppression (Hunt et al., 2013). Identifying the critical variables for optimizing the effects of GABAergic interneuron grafts on seizures is an important area for future investigation.

Some insights can be gained by examining the distributions and/or cell types in different layers of the DG to evaluate whether particular interneuron subtypes are more effective for seizure suppression. Prior research has shown that GABAergic interneurons are highly susceptible to degeneration in MTLE (de Lanerolle et al., 1989) and that surviving SOM^+ interneurons undergo extensive sprouting (Zhang et al., 2009; Thind et al., 2010; Buckmaster and Wen, 2011; Long et al., 2011; Peng et al., 2013). The SOM^+ GABAergic interneurons of the hilus are involved in limiting the initiation of seizures as they are recruited by a feedback mechanism during increases in excitation in the circuitry. By contrast, PV^+ interneurons have a more dominant role in limiting seizure propagation due to their strong feedforward inhibition onto principle cells in the hippocampal circuit (Freund et al., 1992). Our observation that hilar grafts of MGE cells resulted in fewer seizures overall is consistent with an increase in feedback inhibition onto GCs. Our findings showing reductions in generalized seizures in TLE mice with hilar grafts of MGE cells are consistent with increased feedforward inhibition by transplanted PV^+ interneurons. Our analyses, however, showed that transplanted GABAergic interneurons expressing PV, SOM, NPY, CB, or CR migrated throughout the DG with some cells migrating as far as CA1–CA3 pyramidal layers. Within the DG, approximately one-half of the transplanted interneurons coexpressed CB and they were distributed throughout all layers of the DG. Both PV^+ and SOM^+ interneurons comprised the second largest populations of engrafted cell types in the GCL and molecular layers where they established dense axonal projections onto the GC somas and dendrites.

We have shown functionality of the new inhibitory synapses by optogenetically activating ChR2-expressing GABAergic interneurons transplanted into the hippocampus of TLE mice while simultaneously recording from nearby GCs. Depolarizing the transplanted GABAergic interneurons produced immediate and robust hyperpolarizing currents in GCs located within their vicinity, verifying direct and functional synapses between the transplanted interneurons and GCs. We further evaluated transplant-derived inhibitory synaptic function by combining electrophysiological recordings, biocytin staining, and immunohistochemical analyses of postsynaptic molecules. These electrophysiological and confocal microscopic analyses showed that the transplanted GABAergic interneurons increased IPSCs in their GC targets, concomitant with the development of inhibitory synapses with GC dendrites and somas.

To determine whether the SOM^+ or PV^+ subtypes of transplanted GABAergic interneurons mediate different effects in GCs, by example increasing feedback inhibition, feedforward inhibition, or both, it will be necessary to selectively activate or inactivate them experimentally. Such studies might include pharmacological manipulations of designer receptors exclusively activated by designer drugs (DREADDs) to selectively inactivate GABAergic interneuron subtypes after transplantation.

GABAergic synaptic transmission requires clustering of the scaffolding protein gephyrin to regulate $GABA_A$ receptor subunit targeting and localization at sites of inhibitory synapses. In TLE, gephyrin expression is downregulated in hippocampal GCs (Fang et al., 2011; González et al., 2013). Our finding that large postsynaptic clusters of gephyrin molecules had formed within the dendrites and cell bodies of GCs receiving direct input from the transplanted interneurons suggests that the transplants could induce changes in GABA receptor trafficking in dentate GCs. Further insights may be gained by examining GABA receptor subunit expression in GCs receiving input from the transplanted interneurons or by determining whether MGE transplants increase tonic, as well as phasic GABAergic inhibition and thereby reduce dentate GC hyperexcitability.

In summary, our findings suggest that GABAergic progenitor grafts rewire hyperexcitable GC networks in TLE, and that these changes modify the severity and incidence of seizures. As hyperexcitable GCs act as key cellular players contributing to epileptogenesis and SRS (Scharfman et al., 2000, 2003; Danzer, 2008) it will be important to conduct studies in intact rodents with TLE to directly test whether experimental manipulation of inhibitory neural circuits derived from transplanted interneurons regulates seizure activity.

References

Alvarez-Dolado M, Calcagnotto ME, Karkar KM, Southwell DG, Jones-Davis DM, Estrada RC, Rubenstein JL, Alvarez-Buylla A, Baraban SC (2006) Cortical inhibition modified by embryonic neural precursors grafted into the postnatal brain. J Neurosci 26:7380–7389. CrossRef Medline

Baraban SC, Southwell DG, Estrada RC, Jones DL, Sebe JY, Alfaro-Cervello C, García-Verdugo JM, Rubenstein JL, Alvarez-Buylla A (2009) Reduction of seizures by transplantation of cortical GABAergic interneuron precursors into Kv1.1 mutant mice. Proc Natl Acad Sci U S A 106:15472–15477. CrossRef Medline

Buckmaster PS, Dudek FE (1997) Network properties of the dentate gyrus in epileptic rats with hilar neuron loss and granule cell axon reorganization. J Neurophysiol 77:2685–2696. Medline

Buckmaster PS, Lew FH (2011) Rapamycin suppresses mossy fiber sprouting but not seizure frequency in a mouse model of temporal lobe epilepsy. J Neurosci 31:2337–2347. CrossRef Medline

Buckmaster PS, Wen X (2011) Rapamycin suppresses axon sprouting by somatostatin interneurons in a mouse model of temporal lobe epilepsy. Epilepsia 52:2057–2064. CrossRef Medline

Buckmaster PS, Ingram EA, Wen X (2009) Inhibition of the mammalian target of rapamycin signaling pathway suppresses dentate granule cell axon sprouting in a rodent model of temporal lobe epilepsy. J Neurosci 29:8259–8269. CrossRef Medline

Calcagnotto ME, Zipancic I, Piquer-Gil M, Mello LE, Alvarez-Dolado M (2010a) Grafting of GABAergic precursors rescues deficits in hippocampal inhibition. Epilepsia 51:66–70. CrossRef Medline

Calcagnotto ME, Ruiz LP, Blanco MM, Santos-Junior JG, Valente MF, Patti C, Frussa-Filho R, Santiago MF, Zipancic I, Alvarez-Dolado M, Mello LE, Longo BM (2010b) Effect of neuronal precursor cells derived from medial ganglionic eminence in an acute epileptic seizure model. Epilepsia 51:71–75. CrossRef Medline

Carpentino JE, Hartman NW, Grabel LB, Naegele JR (2008) Region-specific differentiation of embryonic stem cell-derived neural progenitor transplants into the adult mouse hippocampus following seizures. J Neurosci Res 86:512–524. CrossRef Medline

Curia G, Longo D, Biagini G, Jones RS, Avoli M (2008) The pilocarpine model of temporal lobe epilepsy. J Neurosci Methods 172:143–157. CrossRef Medline

Danzer SC (2008) Postnatal and adult neurogenesis in the development of human disease. Neuroscientist 14:446–458. CrossRef Medline

Danzer SC, He X, Loepke AW, McNamara JO (2010) Structural plasticity of dentate granule cell mossy fibers during the development of limbic epilepsy. Hippocampus 20:113–124. CrossRef Medline

de Lanerolle NC, Kim JH, Robbins RJ, Spencer DD (1989) Hippocampal interneuron loss and plasticity in human temporal lobe epilepsy. Brain Res 495:387–395. CrossRef Medline

de Lanerolle NC, Kim JH, Williamson A, Spencer SS, Zaveri HP, Eid T, Spencer DD (2003) A retrospective analysis of hippocampal pathology in human temporal lobe epilepsy: evidence for distinctive patient subcategories. Epilepsia 44:677–687. CrossRef Medline

de Lanerolle NC, Lee TS, Spencer D (2012) Histopathology of human epilepsy. In: Jasper's basic mechanisms of the epilepsies, Ed 4, (Noebels JL, Avoli M, Rogawski MA, Olsen RW, Delgado-Escueta AV). Bethesda, MD: National Center For Biotechnology Information.

Fang M, Shen L, Yin H, Pan YM, Wang L, Chen D, Xi ZQ, Xiao Z, Wang XF, Zhou SN (2011) Downregulation of gephyrin in temporal lobe epilepsy neurons in humans and a rat model. Synapse 65:1006–1014. CrossRef Medline

Freund TF, Buzsáki G (1996) Interneurons of the hippocampus. Hippocampus 6:347–470. Medline

Freund TF, Ylinen A, Miettinen R, Pitkänen A, Lahtinen H, Baimbridge KG, Riekkinen PJ (1992) Pattern of neuronal death in the rat hippocampus after status epilepticus: relationship to calcium binding protein content and ischemic vulnerability. Brain Res Bull 28:27–38. CrossRef Medline

Germain ND, Banda EC, Becker S, Naegele JR, Grabel LB (2013) Derivation and isolation of NKX2.1-positive basal forebrain progenitors from human embryonic stem cells. Stem Cells Dev 22:1477–1489. CrossRef Medline

Gernert M, Thompson KW, Löscher W, Tobin AJ (2002) Genetically engineered GABA-producing cells demonstrate anticonvulsant effects and long-term transgene expression when transplanted into the central piriform cortex of rats. Exp Neurol 176:183–192. CrossRef Medline

González MI, Cruz Del Angel Y, Brooks-Kayal A (2013) Down-regulation of gephyrin and GABAA receptor subunits during epileptogenesis in the CA1 region of hippocampus. Epilepsia 54:616–624. CrossRef Medline

Hartman NW, Carpentino JE, LaMonica K, Mor DE, Naegele JR, Grabel L (2010) CXCL12-mediated guidance of migrating embryonic stem cell-derived neural progenitors transplanted into the hippocampus. PloS One 5:e15856. CrossRef Medline

Houser CR (1990) Granule cell dispersion in the dentate gyrus of humans with temporal lobe epilepsy. Brain Res 535:195–204. CrossRef Medline

Hunt RF, Girskis KM, Rubenstein JL, Alvarez-Buylla A, Baraban SC (2013) GABA progenitors grafted into the adult epileptic brain control seizures and abnormal behavior. Nat Neurosci 16:692–697. CrossRef Medline

Kriegstein A, Alvarez-Buylla A (2009) The glial nature of embryonic and adult neural stem cells. Annu Rev Neurosci 32:149–184. CrossRef Medline

Kumar SS, Buckmaster PS (2006) Hyperexcitability, interneurons, and loss

of GABAergic synapses in entorhinal cortex in a model of temporal lobe epilepsy. J Neurosci 26:4613–4623. CrossRef Medline

Long L, Xiao B, Feng L, Yi F, Li G, Li S, Mutasem MA, Chen S, Bi F, Li Y (2011) Selective loss and axonal sprouting of GABAergic interneurons in the sclerotic hippocampus induced by LiCl-pilocarpine. Int J Neurosci 121:69–85. CrossRef Medline

Maisano X, Litvina E, Tagliatela S, Aaron GB, Grabel LB, Naegele JR (2012) Differentiation and functional incorporation of embryonic stem cell-derived GABAergic interneurons in the dentate gyrus of mice with temporal lobe epilepsy. J Neurosci 32:46–61. CrossRef Medline

Margerison JH, Corsellis JA (1966) Epilepsy and the temporal lobes: a clinical, electroencephalographic and neuropathological study of the brain in epilepsy, with particular reference to the temporal lobes. Brain 89:499–530. CrossRef Medline

Maroof AM, Keros S, Tyson JA, Ying SW, Ganat YM, Merkle FT, Liu B, Goulburn A, Stanley EG, Elefanty AG, Widmer HR, Eggan K, Goldstein PA, Anderson SA, Studer L (2013) Directed differentiation and functional maturation of cortical interneurons from human embryonic stem cells. Cell Stem Cell 12:559–572. CrossRef Medline

Mathern GW, Babb TL, Vickrey BG, Melendez M, Pretorius JK (1995) The clinical-pathogenic mechanisms of hippocampal neuron loss and surgical outcomes in temporal lobe epilepsy. Brain 118:105–118. CrossRef Medline

Mazzuferi M, Kumar G, Rospo C, Kaminski RM (2012) Rapid epileptogenesis in the mouse pilocarpine model: video-EEG, pharmacokinetic and histopathological characterization. Exp Neurol 238:156–167. CrossRef Medline

Murphy BL, Pun RY, Yin H, Faulkner CR, Loepke AW, Danzer SC (2011) Heterogeneous integration of adult-generated granule cells into the epileptic brain. J Neurosci 31:105–117. CrossRef Medline

Nadler JV (2003) The recurrent mossy fiber pathway of the epileptic brain. Neurochem Res 28:1649–1658. CrossRef Medline

Nait Oumesmar B, Vignais L, Baron-Van Evercooren A (1997) Developmental expression of platelet-derived growth factor alpha-receptor in neurons and glial cells of the mouse CNS. J Neurosci 17:125–139. Medline

Nicholas CR, Chen J, Tang Y, Southwell DG, Chalmers N, Vogt D, Arnold CM, Chen YJ, Stanley EG, Elefanty AG, Sasai Y, Alvarez-Buylla A, Rubenstein JL, Kriegstein AR (2013) Functional maturation of hPSC-derived forebrain interneurons requires an extended timeline and mimics human neural development. Cell Stem Cell 12:573–586. CrossRef Medline

Paxinos GF, Franklin, KB (2008) The mouse brain in stereotaxic coordinates, Ed 3. San Diego: Academic.

Peng Z, Zhang N, Wei W, Huang CS, Cetina Y, Otis TS, Houser CR (2013) A reorganized GABAergic circuit in a model of epilepsy: evidence from optogenetic labeling and stimulation of somatostatin interneurons. J Neurosci 33:14392–14405. CrossRef Medline

Scharfman HE, Pierce JP (2012) New insights into the role of hilar ectopic granule cells in the dentate gyrus based on quantitative anatomic analysis and three-dimensional reconstruction. Epilepsia 53:109–115. CrossRef Medline

Scharfman HE, Goodman JH, Sollas AL (2000) Granule-like neurons at the hilar/CA3 border after status epilepticus and their synchrony with area CA3 pyramidal cells: functional implications of seizure-induced neurogenesis. J Neurosci 20:6144–6158. Medline

Scharfman HE, Sollas AE, Berger RE, Goodman JH, Pierce JP (2003) Perforant path activation of ectopic granule cells that are born after pilocarpine-induced seizures. Neuroscience 121:1017–1029. CrossRef Medline

Schoenenberger P, Schärer YPZ, Oertner TG (2011) Channelrhodopsin as a tool to investigate synaptic transmission and plasticity. Exp Physiol 96:34–39. CrossRef Medline

Shibley H, Smith BN (2002) Pilocarpine-induced status epilepticus results in mossy fiber sprouting and spontaneous seizures in C57BL/6 and CD-1 mice. Epilepsy Res 49:109–120. CrossRef Medline

Swartz BE, Houser CR, Tomiyasu U, Walsh GO, DeSalles A, Rich JR, Delgado-Escueta A (2006) Hippocampal cell loss in posttraumatic human epilepsy. Epilepsia 47:1373–1382. CrossRef Medline

Tauck DL, Nadler JV (1985) Evidence of functional mossy fiber sprouting in hippocampal formation of kainic acid-treated rats. J Neurosci 5:1016–1022. Medline

Thind KK, Yamawaki R, Phanwar I, Zhang G, Wen X, Buckmaster PS (2010) Initial loss but later excess of GABAergic synapses with dentate granule cells in a rat model of temporal lobe epilepsy. J Comp Neurol 518:647–667. CrossRef Medline

Thompson K (2009) Transplantation of GABA-producing cells for seizure control in models of temporal lobe epilepsy. Neurotherapeutics 6:284–294. CrossRef Medline

Tóth K, Eross L, Vajda J, Halász P, Freund TF, Maglóczky Z (2010) Loss and reorganization of calretinin-containing interneurons in the epileptic human hippocampus. Brain 133:2763–2777. CrossRef Medline

Tyson JA, Anderson SA (2014) GABAergic interneuron transplants to study development and treat disease. Trends Neurosci 37:169–177. CrossRef Medline

Waldau B, Hattiangady B, Kuruba R, Shetty AK (2010) Medial ganglionic eminence-derived neural stem cell grafts ease spontaneous seizures and restore GDNF expression in a rat model of chronic temporal lobe epilepsy. Stem Cells 28:1153–1164. CrossRef Medline

Walter C, Murphy BL, Pun RY, Spieles-Engemann AL, Danzer SC (2007) Pilocarpine-induced seizures cause selective time-dependent changes to adult-generated hippocampal dentate granule cells. J Neurosci 27:7541–7552. CrossRef Medline

Wang H, Peca J, Matsuzaki M, Matsuzaki K, Noguchi J, Qiu L, Wang D, Zhang F, Boyden E, Deisseroth K, Kasai H, Hall WC, Feng G, Augustine GJ (2007) High-speed mapping of synaptic connectivity using photostimulation in Channelrhodopsin-2 transgenic mice. Proc Natl Acad Sci U S A 104:8143–8148. CrossRef Medline

Wang Y, Kakizaki T, Sakagami H, Saito K, Ebihara S, Kato M, Hirabayashi M, Saito Y, Furuya N, Yanagawa Y (2009) Fluorescent labeling of both GABAaergic and glycinergic neurons in vesicular GABA transporter (VGAT)-Venus transgenic mouse. Neuroscience 164:1031–1043. CrossRef Medline

Wichterle H, Garcia-Verdugo JM, Herrera DG, Alvarez-Buylla A (1999) Young neurons from medial ganglionic eminence disperse in adult and embryonic brain. Nat Neurosci 2:461–466. CrossRef Medline

Woodruff RH, Tekki-Kessaris N, Stiles CD, Rowitch DH, Richardson WD (2001) Oligodendrocyte development in the spinal cord and telencephalon: common themes and new perspectives. Int J Dev Neurosci 19:379–385. CrossRef Medline

Xu Q, Cobos I, De La Cruz E, Rubenstein JL, Anderson SA (2004) Origins of cortical interneuron subtypes. J Neurosci 24:2612–2622. CrossRef Medline

Zhang W, Yamawaki R, Wen X, Uhl J, Diaz J, Prince DA, Buckmaster PS (2009) Surviving hilar somatostatin interneurons enlarge, sprout axons, and form new synapses with granule cells in a mouse model of temporal lobe epilepsy. J Neurosci 29:14247–14256. CrossRef Medline

Zhao S, Ting JT, Atallah HE, Qiu L, Tan J, Gloss B, Augustine GJ, Deisseroth K, Luo M, Graybiel AM, Feng G (2011) Cell type-specific channelrhodopsin-2 transgenic mice for optogenetic dissection of neural circuitry function. Nat Methods 8:745–752. CrossRef Medline

Zipancic I, Calcagnotto ME, Piquer-Gil M, Mello LE, Alvarez-Dolado M (2010) Transplant of GABAergic precursors restores hippocampal inhibitory function in a mouse model of seizure susceptibility. Cell Transplantation 19:549–564. CrossRef Medline